

Estimation of mean atmospheric turbidity coefficient in Makurdi, Nigeria

Yusuf SD^{1*}, Lumbi WL², Loko ZA³, Usaka IG⁴

¹⁻⁴ Department of Physics, Faculty of Natural and Applied Sciences, Nasarawa State University, Keffi, Nigeria

Abstract

For effective development of solar energy devices and estimation of their performance efficiencies, knowledge of the solar radiation available on the earth's surface is of utmost important. This study estimated the atmospheric turbidity coefficient and extinction coefficient in Makurdi for the period of five years (2010-2014) using data of visibility obtained from the Nigeria Meteorological Agency of The Tactical Air Force Command, Makurdi. Monthly average values of turbidity coefficient and extinction coefficient were estimated using the Schuepp's empirical formula and the Koschmeida formula respectively. Result shows that the monthly average turbidity coefficient ranges between 0.266 and 0.235 while the monthly average extinction coefficient ranges between 0.271 and 0.542. These values were high especially in January, February and December during the dry season, and low in March during the rainy season. The atmospheric turbidity coefficient is important for technological utilization of solar energy and for the purposes of meteorology, ecology, climatology and monitoring of atmospheric pollution.

Keywords: turbidity coefficient, visibility, extinction coefficient, atmosphere, schuepp's method, koschmeida method

1. Introduction

The study of solar energy availability in many areas of the world has been attributed to the increase in terrestrial applications of solar radiant energy ^[1]. For the development of solar energy devices and estimation of their performance efficiencies a knowledge of the solar radiation available on the earth's surface is of utmost important. However, according to Robaa *et al.* ^[2] not all solar radiation received at the periphery of the atmosphere reaches the Earth's surface. Solar radiation is partially depleted and attenuated as it traverses the atmospheric layers ^[3]. According to Elminir *et al.* ^[1], extra-terrestrial solar radiation when passing through the earth's atmosphere is usually subjected to attenuation due to scattering by the air molecules and aerosols, and also due to absorption by various atmospheric components mainly ozone, water vapour, oxygen and carbon dioxide. An important factors that affect or attenuates the amount of solar radiation that reaches the Earth's surface under cloudless skies is the presence of aerosol particles in the atmosphere as a measure of atmospheric turbidity ^[4, 5]. Thus, atmospheric aerosol load have been explained to be associated with atmospheric turbidity ^[2]. In line with this, an atmosphere that contains aerosols is described as turbid or hazy ^[6]. Elminir *et al.* ^[1] had posit that; the extinction of the radiation is strongly dependent on the state of the sky which include cleanliness of the atmosphere, whether cloudy or not, and the amount of gaseous absorbers. Elminir *et al.* ^[1] added that for technological utilization of solar energy, a study of solar radiation under cloudless skies is very important.

Rangarajan and Mani ^[7] defined atmospheric turbidity as a measure of the total vertically integrated particulate load in the atmosphere, an important factor influencing the energetics of solar radiation in the earth's atmosphere. Djafer and Irbah ^[8] added that atmospheric turbidity expresses the attenuation of the solar radiation that reaches the Earth's surface under cloudless sky and describes the optical thickness of the atmosphere. It is a useful index of

atmospheric pollution, particularly in studies of long-term secular changes in the composition of the atmosphere and resultant global climatic changes. However, despite its importance, there does not appear to be any universally-adopted definition of turbidity or any universally-accepted technique for its measurement ^[7]. According to Rahoma and Hassan ^[9] the study of Atmospheric turbidity is important for purposes of meteorology, ecology, climatology and monitoring of atmospheric pollution. However, since atmospheric turbidity characterizes the extinction effect of aerosols on solar radiation, Gueymard ^[10] explained that turbidity affects the direct and diffuse components of solar radiation under clear skies and that, as turbidity increases, the direct radiation decreases and the diffuse radiation increases in about the same proportions so that the total effect of turbidity on global radiation is considerably smaller.

According to Lopez and Batlles ^[5] aerosols are solid and liquid particles suspended in the atmosphere, ranging in size from 10^{-3} μm to several tens of microns either of natural sources (such as volcanic eruptions, dust storms, forest and grassland fires, sea spray, etc.) or of anthropogenic origin (such as the burning of fossil fuels). In the case of Makurdi in Benue State, Nigeria, the major source of aerosols is of anthropogenic origin (burning of fossil fuels) due to the availability of industries including Nigerian National Petroleum Company Depot, rice meal, cassava mills and some other grain mills. According to Eltabaakh *et al.* ^[11] aerosols have direct radiative forcing because they scatter and absorb solar and infrared radiations in the atmosphere as well as alter warm, ice, and mixed-phase cloud formation processes by increasing droplet concentrations and ice particle concentrations, consequently causing indirect radiative forcing associated with the changes in the microphysical and optical properties of clouds. Lopez and Batlles ^[5] added that an increase in the concentration of aerosols in some urban regions caused by human activity has a significant impact on the environmental quality of the

cities, which makes the atmospheric opto-chemistry faster, the air turbid with lower visibility, and polluted. Eltabaakh *et al.* [11] explained further that; aerosols are highly absorbent of solar radiation, such as black carbon, and they may reduce cloud cover and liquid water contents by heating the cloud and the environment where the cloud forms. This is known as the semi-direct effect because it is the result of the direct interaction of aerosols with radiation that indirectly influences the climate by altering clouds. The net effect of aerosols on climate depends on the summation of all the three mechanisms above [12]. However, aerosols have two dominant layers in the atmosphere. According to Lopez and Batlles [5] the first dominant layer is near the Earth's surface at 0–3 km, which is affected by natural dust storms and man-made inputs to the atmosphere, whereas the second dominant layer is the stratospheric dust layer at 15–25 km above sea level, which is caused by volcanic action and cosmic sources. In addition, aerosols play an important role in absorption and scattering of solar radiation, as well as in the physics of clouds and precipitation [5].

A key reason for the uncertainty about aerosols-climate interaction is that aerosols demonstrate high variability, both spatially and temporally and that the extent of their variability has not been fully investigated [13]. There is a paucity of reliable data on the amount of aerosols in the atmosphere. Conventional techniques for quantifying atmospheric turbidity the amount of aerosol integrated vertically through the atmosphere typically require costly and sophisticated instrumentation and clear-sky condition [14, 15]. Recent satellite estimates of turbidity are also restricted to clear-sky condition and non-terrestrial region [16, 17]. The clear-sky restriction produces gaps in the turbidity record, as well as a possible bias because cloudless skies are associated with a limited set of synoptic situation. In addition to these potential biases, atmospheric turbidity measurements and estimation are not optimally distributed in space, they are geographically biased [13].

Due to the relationship existing between aerosols and attenuation of solar radiation reaching the Earth's surface, different turbidity factors based on radiometric methods have been defined to evaluate the atmospheric turbidity. Some of these are the Linke's turbidity factor, T_l [18], the Angstrom turbidity parameters, β [19], the Schuepp coefficient, B [20], the Unsworth-Monteith turbidity factor, T_u [21] others methods are Illuminance turbidity coefficient, T_{il} , Volz turbidity coefficient, T_v , and Kastrov turbidity coefficient, T_k . In this study, the Schuepp method was adapted to measure the atmospheric turbidity coefficient while the Koschmeida method was employed to calculate the extinction coefficient for the city of Markurdi Nigeria using the visibility data for the period of five years (2010-2014) from Nigeria Meteorological Headquarters Tactical Air Command Makurdi Airport.

Atmospheric turbidity is a useful index of atmospheric pollution particularly in studies of long-term secular changes in the composition of the atmosphere and the resultant global climate change [22]. It is affected by amount, kind and size distribution of aerosols as well as the amount and distribution of atmospheric water vapour [23]. Measurement of atmospheric turbidity is important in meteorology, climatology, atmospheric pollution, and in determining the amount of spectral global irradiance and for designing photovoltaic cells.

2. Literature Review

The knowledge of atmospheric turbidity, as a measure of aerosols load, is important for the estimation of the impact of a polluted atmosphere on weather and climate, studying air pollution and energy exchange, correcting satellite image for the atmosphere effect in the visible spectral range (especially over polluted regions), and simulating spectral solar irradiance which is helpful in the design of photovoltaics, window glazing for energy-efficient buildings, calculation of heating and cooling loads in architecture and the design of flat-plate collectors [24, 25]. Several empirical models have been developed to calculate atmospheric turbidity coefficient using various parameters [26, 27, 28, 29, 21, 30, 31].

Angstrom in [19] developed the earliest model used for estimating turbidity coefficient (β). He defined it as a dimensionless index that represents the amount of aerosols in the vertical column or direction. In addition, it represents the combined effects of both scattering and absorption caused by aerosols [25]. This representation of atmospheric turbidity by Angstrom is very common. According to Katz *et al.* [24] its determination has been subjected to a number of projects. The minimum value (zero) refers to an ideally dust free atmosphere, while values superior to unity refers to an extremely turbid atmosphere. Under clear sky conditions, an atmosphere aerosol generally contributes to the largest attenuation of solar radiation in the visible region. Scattering and absorption effects are caused by aerosols [26, 27].

Angstrom model is given as $T_{a\lambda} = \beta\lambda^\alpha$ where β is an index which is the amount of aerosols in the atmosphere at the vertical direction and varies from 0.0 to 0.5 or even higher [6]. The wavelength exponent α is related to the size distribution of the aerosols particles, large values of α indicates a relatively high ratio of small to large particles.

Linke in [18] forwarded the ideal of turbidity, eventually named the Linke's factor and it was defined as the number of clean and dry atmosphere that would be necessary to produce the same attenuation of extra-terrestrial solar radiation that is produced by the real atmosphere [29]. It was suggested that Linke's turbidity coefficient is not a pure turbidity coefficient because it also incorporates water vapour and NO_2 optical depth. Nevertheless, the turbidity may be useful when no data on precipitable water are available making the determination of other coefficient difficult. Although Linke does not explicitly show the effects of aerosols and water vapour, its easy measurement made it quite popular in meteorological station [32]. Linke's turbidity is a key input for several models that assess the downwelling irradiance under clear skies. These models are used by several communities in the field of renewable energies, climatology, argo-meteorological and atmospheric pollution. Linke turbidity coefficient is also useful for the prediction of the availability of solar radiation. It has a serious drawback; it varies with air mass even when atmospheric condition remains constant. Linke can be directly linked obtained from the pyrheliometric measurements of the beam irradiance during periods of very clear sky with an air mass of 2. Since this kind of data is rarely available, Linke's turbidity generally becomes an estimated parameter. In addition, the time series of the radiation data is generally too short to allow estimation on a daily basis. Fortunately, long-term monthly averages values are sufficient for most applications. Attempts have been made to relate it to Angstrom turbidity [28].

Unsworth and Monteith [21] had introduced a method for estimating of turbidity of the atmosphere. The Unsworth-Monteith turbidity represents the number of clean and dry atmosphere which exhibits the same attenuation as the actual atmosphere that contains aerosols and water vapour. They used experimental irradiance measurements of a clean atmosphere and developed the formula $I_{bn,\lambda} = I_{bn,\lambda} \exp(-T_{U\lambda} m_r)$ where I_{bn} and m_r represents the normal incidence total solar radiation under a dust-free atmosphere (Wm^{-2}), and $\exp(-T_u m_r)$ represents an aerosol spectral transmittance coefficient. With the definition of the integrated total optical thickness, an integrated expression of T_u that is similar to the expression of T_i given as $T_u = \frac{1}{m_r} \ln(\frac{I_{bn}}{I_{bn0}})$

Illuminance turbidity factor was introduced by Navvab *et al.* [31]. The concept of the illuminance turbidity factor is analogous to that of the Linke factor with I_{bn} , I_0 , and T_u substituted with I_{vsn} , I_{v0} , and T_{il} . The turbidity is apparently a better parameter for describing atmospheric conditions because, unlike the Linke factor, it is insensitive to water vapour content, airmass, and solar altitude angle or time of day. It can be determined from the direct measurement of the beam normal illuminance. Illuminance turbidity can be given as $T_{il} (\frac{1}{\delta_{il} m_r}) \ln(\frac{I_{vsn}}{I_{v0}})$ where the values of δ_{il} can be calculated as $\delta_{il} = \frac{0.1}{1+0.0045 m_r}$. Illuminance turbidity has a heuristic advantage as an approximate analytical expression because it can be directly derived from the Angstrom turbidity formula given as $T_{il} = 1 + 21.6\beta$.

Computations of Volz's turbidity are performed according to the usual Bouguer-Lambert-Beer Law that expresses the measured intensity at wavelength λ given as $T_v = \left[\frac{\ln I_{bn} - \ln I_0 - \ln L_0}{m_r} \right] - T_a^R - T_a^W$ where T_a^R is the Rayleigh scattering coefficient for air molecules at wavelength λ , and T_a^W is the absorption coefficient for ozone at λ .

Adeyefa *et al.* [33] reports that Kastrov [34] obtained the following simple formula for the integral solar radiation on surface level as $I_b = \frac{I_{sc}}{1+T_k m_r}$ from which we obtain $T_k = \frac{1}{m} * (\frac{I_{sc}}{I_b} - 1)$ where T_k is a quantitative characteristic of atmospheric transparency.

Majumda *et al.* [30] defined a new measure of total atmospheric turbidity, termed as the rational turbidity coefficient, T_r , to overcome the limitations of the Linke turbidity Coefficient T_L . It is composed of three components namely,

- (i) Pure and dry air (the basic effect),
- (ii) Perceptible water vapour w, and
- (iii) Aerosol particles in the atmosphere (dust, smoke, and haze).

The formulation for the rational turbidity coefficient is given as $T_r = \frac{1}{m} (\frac{0.3249 - \ln I_{bn}}{0.072375})^{0.57}$. They correlated the rational turbidity coefficient with the Angstrom-Schuepp turbidity coefficient B for different values of perceptible water w at unit airmass to eliminate the effect of any possible virtual variation with airmass. They demonstrated that the effect of B and w were inseparable because the scattering of radiation by aerosol particles and the

absorption of the same by water vapour coexist within the absorption bands of water vapour. Thus, the two effects cannot be isolated from each other. This interaction becomes more pronounced with increasing particle size since the negative exponent of 1 in the Angstrom-Schuepp equation approaches zero for large particles. It also investigated the effects of varying air masses m_r on T_r in relation to B and w and presented a formula that connects T_r with B, w, and m_r as $T_r = 1 + 80(\frac{B}{1.8})^{1+0.817(0.596)m_r} + [25(\frac{B+0.1}{1.9})^{1-0.2247(0.869)m_r}]w^{0.3}$.

Schuepp introduced the turbidity parameter B, which is fundamentally based similarly with β (Angstrom turbidity) because they have the same theoretical basis. $B = 0.25 - 0.017V$ is Schuepps turbidity coefficient and, V is visibility in metres. Hence, an excellent survey of the different sources of error which should be avoided or corrected for on actinometrical research, especially when we wish to determine from such measurement the parameters of atmospheric transmission like turbidity coefficient and the wavelength exponent. However, this is the easiest method in estimating atmospheric turbidity because it does not require much data record.

Angstrom and Schuepp are true turbidity coefficients that are unaffected by anything except by the aerosols total burden. However, Linke turbidity coefficient is affected by the presence of mass aerosols particles in the atmosphere there by causing it to be turbid, effect of perceptible water vapour from absorption, and pure and dry air (basic effect).

3. Materials and Method

The data for this research was obtained from the record section of department of meteorological station of the Tactical Air Command, Makurdi, Benue state, Nigeria. The record section contains daily record for visibility. For the purpose of this research the monthly mean data on visibility in kilometres (km) was retrieved for the period of five years (2010-2014). A typical sample of the data for visibility obtained from NIMET recorded for the period of January to December in the year 2010 is as shown in Appendix. The monthly mean visibility V can be calculated as follows:

$$V = \sum fd/d \tag{I}$$

where f is the frequency and d is the distance in kilometres. The Schuepp's method was employed to calculate the turbidity coefficient B. This is because the Schuepp method gives a true turbidity coefficient that are unaffected by anything except by the aerosols total burden. However, following the work of Excell [35], was obtained the turbidity coefficient as:

$$B = 0.25 - 0.0017V \tag{II}$$

where V is the mean visibility in kilometres. In a similar way, the Koschmeida method was employed to calculate the extinction coefficients b_{ext} and following the work of Dobbins [36], the extinction coefficient is given as:

$$b_{ext} = \frac{3.912}{V} \tag{III}$$

where V is the mean visibility in kilometres

3.1 Study Area

This research was carried out in Makurdi, Benue State Nigeria. The Benue valley covers about 56,980 square kilometres of Nigeria landscape. Makurdi, which is the Capital of Benue State, is situated in this valley at an elevation of 100m above the sea level [5]. The Makurdi climate is found between the equatorial forest and trade wind hot desert, known as Sudan or savannah climate. Makurdi, is located on latitude 07.41°E of the equator and on longitude 08.7°E and has an altitude of 106.4m. The data for this research have been measured and recorded at the department of meteorological services of the tactical air force command Makurdi, which is located at 6km from the centre of Makurdi town along Gboko road.

4. Results

4.1 Mean visibility

The monthly visibility was calculated using equation I. From the data table (appendix) the mean visibility for

January 2010 can be calculated. First 100, 200, 400 metres do not have any observation, but at 1km it had the frequency 3 for the first week, 2 for the second week and 1 each in the third and fourth week which gives a total frequency of 6, then at 2km the total frequency is 11 and 46 for 4km. Between 10-19km, a mean distance of 15km was selected. Thus, the monthly visibility V in km can be calculated as:

$$V = \frac{6 \cdot 1 + 11 \cdot 2 + 43 \cdot 4 + 66 \cdot 15}{126} = \frac{1190}{126} = 9.444 \approx 9.44$$

Similar process was repeated for the rest of the months to obtain the monthly visibility for each year from 2010 – 2014. The average monthly visibility \bar{V} for five years was then calculated. The monthly mean visibility, the annual mean visibility and standard deviation were calculate and the variation of this measured values from 2010 to 2014 are summarized in Table I.

Table 1: 5-year monthly mean visibility (km) and their standard deviation

Months	2010	2011	2012	2013	2014	\bar{V} (km)	S
January	9.44	12.00	NA	6.00	11.20	9.65	4.90
February	8.78	10.00	NA	9.40	9.00	9.30	4.18
March	14.34	13.30	NA	15.00	15.00	14.40	6.48
April	8.24	14.30	NA	15.00	15.00	13.13	6.52
May	14.31	15.00	6.00	15.00	15.00	13.06	6.40
June	14.19	15.00	10.00	14.30	15.00	13.70	5.90
July	14.13	14.10	9.40	14.10	14.10	13.16	5.70
August	13.64	13.00	14.30	14.10	14.00	13.80	5.66
September	10.12	13.30	14.00	15.00	15.00	13.48	5.79
October	13.72	14.00	14.40	15.00	14.10	14.24	5.83
November	14.34	12.00	15.00	15.00	14.00	14.06	5.85
December	9.74	10.20	3.00	14.00	11.30	9.64	5.36
Average	12.08 ± 2.54	13.02 ± 1.68	10.76 ± 4.47	13.49 ± 2.83	13.56 ± 1.97	12.58 ± 1.92	

Note: N A- Not Available, \bar{V} is monthly mean visibility coefficient, S is the standard deviation

From Table I it can be seen that year 2014 recorded the highest annual mean visibility of 13.56 km with standard deviation (1.97) while the lowest annual mean visibility of 10.76 km was obtained in the year 2012 with standard

deviation (4.47) during the 5 years period (2010-2014). The variation of the annual mean visibility is as shown in Figure I.

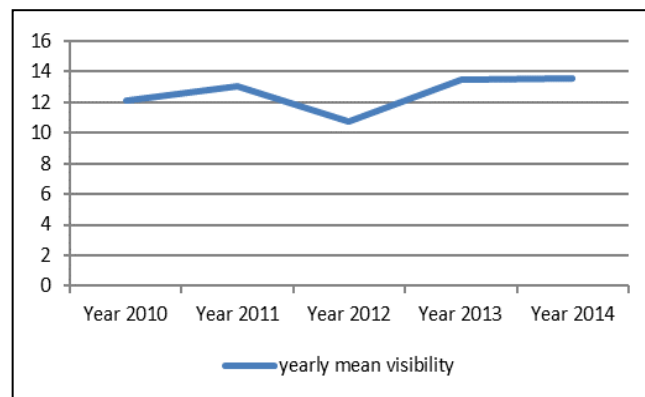


Fig 1: Annual mean visibility

Figure II(a) shows the five years monthly values of visibility from 2010 to 2014. The minimum visibility value of 3km was recorded in December 2012 while maximum visibility value of 15km was found in different months of the years 2011-2014. In the year 2012, from January to April there were no available records during those months. In terms of

the monthly mean visibility values averaged for five years as shown in Figure II(b), it shows that February has a lowest mean visibility value of 9.30 km with standard deviation (4.18) while March has the highest mean visibility of 14.40 km with standard deviation (6.48).

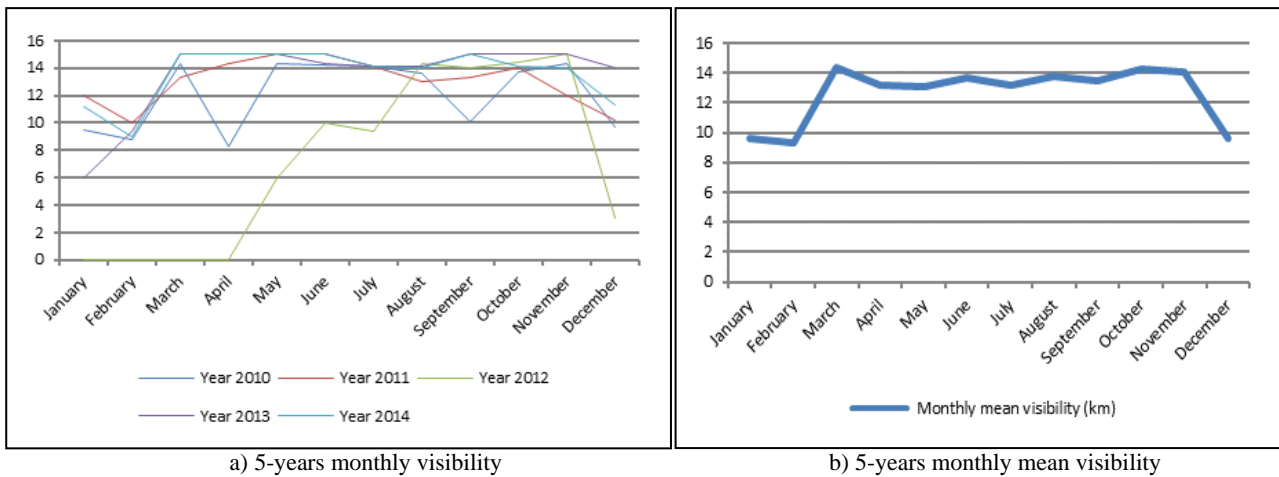


Fig 2: 5-years visibility graph

4.2 Turbidity coefficient

The average monthly turbidity coefficient \bar{B} was calculated using the Schuepp’s method given in equation II following the work of Excell [35]. However, the monthly mean

turbidity coefficient, the annual mean turbidity coefficient and standard deviation were calculate and the variation of this measured values from 2010 to 2014 are summarized in Table II.

Table 2: 5-yearly mean monthly turbidity coefficient and it’s standard deviation

Months	2010	2011	2012	2013	2014	\bar{B} (km)	S
January	0.234	0.230	NA	0.240	0.231	0.234	0.105
February	0.235	0.233	NA	0.234	0.235	0.234	0.105
March	0.226	0.227	NA	0.225	0.225	0.226	0.101
April	0.236	0.226	NA	0.225	0.225	0.228	0.102
May	0.226	0.225	0.240	0.225	0.225	0.228	0.093
June	0.226	0.225	0.233	0.226	0.225	0.227	0.093
July	0.226	0.226	0.234	0.226	0.226	0.228	0.093
August	0.227	0.227	0.226	0.226	0.226	0.226	0.092
September	0.233	0.227	0.226	0.225	0.225	0.227	0.093
October	0.227	0.226	0.226	0.225	0.226	0.226	0.092
November	0.226	0.230	0.225	0.225	0.226	0.226	0.092
December	0.233	0.233	0.250	0.226	0.231	0.235	0.096
Average	0.229 ± 0.004	0.228 ± 0.003	0.233 ± 0.009	0.227 ± 0.005	0.227 ± 0.003	0.229 ± 0.003	

Note: N A- Not Available, \bar{B} is monthly mean turbidity coefficient, S is the standard deviation

From Table II, it shows that year 2012 recorded the highest annual mean turbidity coefficient of 0.233 km with standard deviation (0.009) while the lowest annual mean turbidity coefficient of 0.227 was observed in the year 2013 and 2014 with standard deviations (0.005) and (0.003) respectively. Figure III shows the variation in the annual mean turbidity

coefficient of which we observed that; the pattern of the variation appears to be inversely to the variation in the annual mean visibility as we compare Figure I and III. Therefore, increase in annual mean visibility results in a decrease in annual mean turbidity and vise-versa.

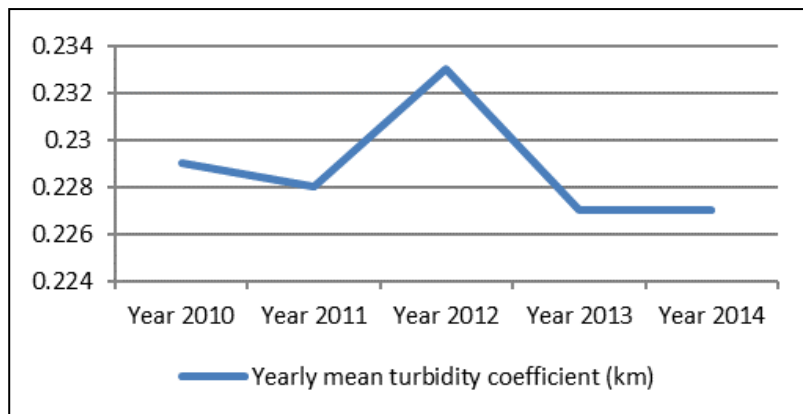


Fig 3: Annual mean turbidity coefficient

Figure IV(a) shows the monthly values of the turbidity coefficient from 2010 to 2014. There was variation in the monthly values with maximum value of 0.250 occurring in December 2012 while the minimum value of 0.225 was found in different months across the years 2011-2014. Again since there were no available records from January to April in the year 2012, there was no any calculated turbidity values associated to those months. Figure IV(b) shows the monthly mean turbidity coefficient values averaged for five years of which we observe that; the pattern of the variation

appears to be inversely to the variation in the mean monthly visibility as we compare Figure II(b) and IV(b). This means that an increase in monthly mean visibility will result in a decrease in the monthly mean turbidity and vice-versa. However, we observe that December had the highest monthly mean turbidity coefficient of 0.235 km with standard deviation (0.096) while the lowest monthly mean turbidity coefficient of 0.226 km was observed in March with standard deviation (0.101), August, October and November with standard deviations (0.092) each.

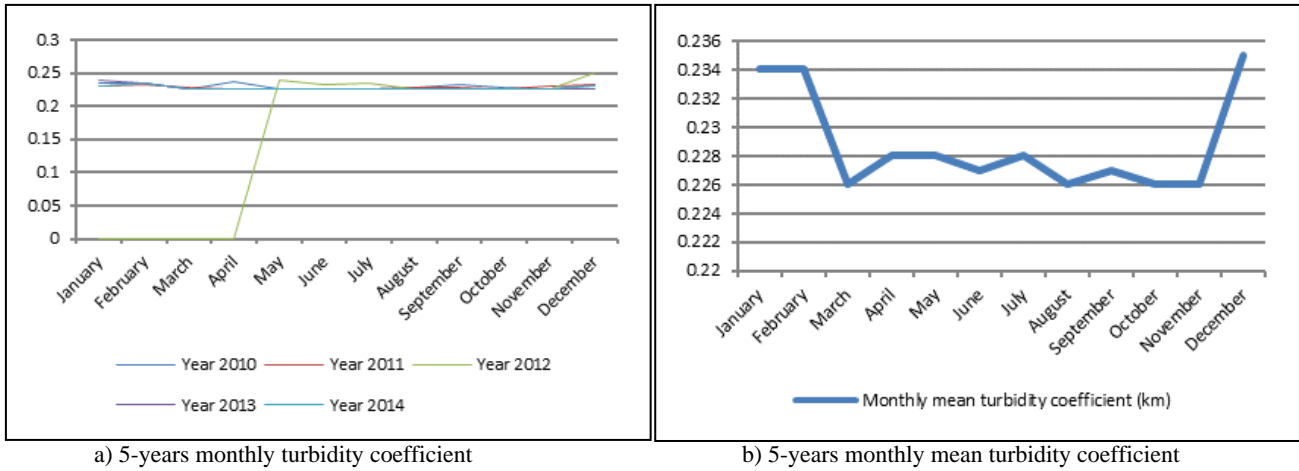


Fig 4: 5-years turbidity coefficient graph

4.3 Extinction coefficient

The monthly extinction coefficient was calculated using the Koschmeida method given in equation III following the work of Dobbins [36]. However, the monthly mean extinction

coefficient, the annual mean extinction coefficient and standard deviation were calculate and the variation of this measured values from 2010 to 2014 are summarized in Table III.

Table 3: Extinction coefficient monthly mean (km^{-1})

Months	2010	2011	2012	2013	2014	$\bar{b}_{ext} (km^{-1})$	S
January	0.414	0.330	NA	0.650	0.350	0.436	0.233
February	0.446	0.390	NA	0.420	0.440	0.424	0.191
March	0.273	0.290	NA	0.260	0.260	0.271	0.122
April	0.475	0.270	NA	0.260	0.260	0.316	0.169
May	0.273	0.260	0.650	0.260	0.260	0.341	0.208
June	0.276	0.260	0.390	0.270	0.260	0.291	0.129
July	0.277	0.280	0.420	0.280	0.280	0.307	0.138
August	0.287	0.300	0.270	0.280	0.280	0.283	0.116
September	0.387	0.290	0.280	0.260	0.260	0.295	0.129
October	0.285	0.280	0.270	0.260	0.280	0.275	0.113
November	0.273	0.330	0.260	0.260	0.280	0.281	0.117
December	0.402	0.380	1.300	0.280	0.350	0.542	0.441
Average	0.339 ± 0.079	0.305 ± 0.044	0.480 ± 0.356	0.312 ± 0.116	0.297 ± 0.056	0.339 ± 0.085	

Note: N A- Not Available, \bar{b}_{ext} is monthly mean extinction coefficient, S is the standard deviation

From Table II, it shows that year 2012 recorded the highest annual mean extinction coefficient of 0.480 km with standard deviation (0.356) while the lowest annual mean turbidity coefficient of 0.297 with standard deviation (0.056), was observed in the year 2014. Figure V shows the variation in the annual mean extinction coefficient of which we observed that the pattern of the variation is similar to the variation in the annual mean turbidity as we compare Figure III and V. Therefore, increase in annual mean turbidity coefficient results in a increase in annual mean extinction coefficient and vice-versa.

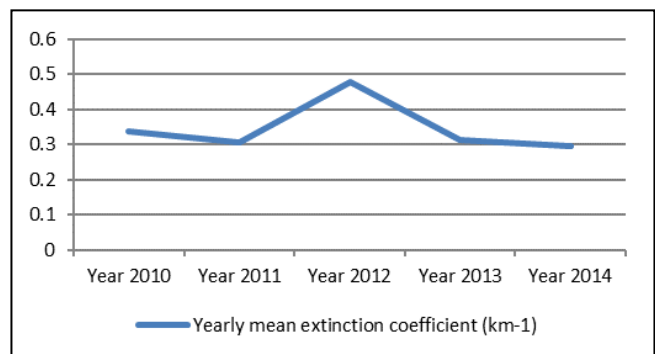


Fig 5: Annual mean extinction coefficient

Figure VI(a) shows the monthly values of the extinction coefficient from 2010 to 2014. There was also variation in the monthly values with maximum value of 1.30 occurring in December 2012 while the minimum value of 0.26 was found in different months across the years 2011-2014. Again since there were no available records from January to April in the year 2012, there was no any calculated extinction values associated to those months. Figure VI(b) shows the monthly mean extinction coefficient values averaged for five years of which we observe that; the pattern

of the variation appears to be similar to the variation in the mean monthly turbidity as we compare Figure IV(b) and VI(b). This also implies that an increase in the monthly mean turbidity coefficient will result in an increase in monthly mean extinction coefficient and vice-versa. However, we observe that December had the highest monthly mean extinction coefficient of 0.542 km with standard deviation (0.441) while the lowest monthly mean extinction coefficient of 0.271 km with standard deviation (0.122) was observed in March.

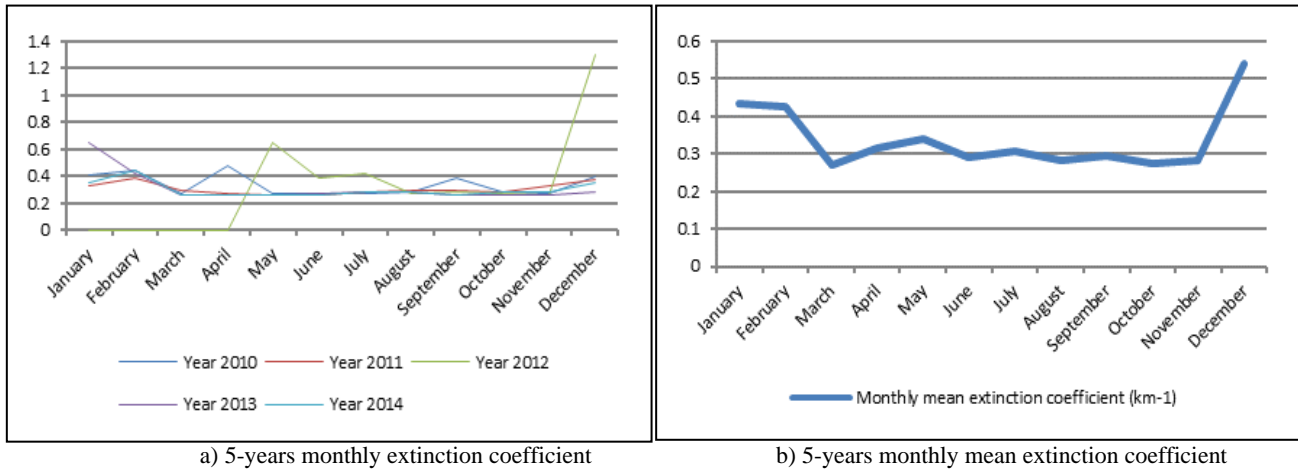


Fig 6: 5-years extinction coefficient graph

4.4 Comparison of estimated turbidity and extinction coefficients results

Table IV is a comparison of the monthly mean turbidity and extinction coefficient averaged over five years as represented in Figure VII. The monthly mean extinction coefficients averaged over five years appears to be similar but higher than those of the turbidity coefficients. This values are observed to show considerable variation across the months as compared to the monthly mean turbidity coefficients that shows little or no variation across the months for the five years average. The monthly mean

coefficient shows that the turbidity coefficients for the months of January, February and December have high values 0.234km, 0.234km and 0.235km each respectively. Showing that aerosole loading is much higher during the dry season. Correspondingly, the extinction coefficient has an average values of 0.436 km^{-1} , 0.424 km^{-1} and 0.542 km^{-1} respectively during these months. On the other hand, during the rainy season, low values of turbidity up to about 0.226km are observed and the extinction coefficients up to 0.271 km^{-1} are observed showing low aerosole loading.

Table 4: Visibility, turbidity coefficient and extinction coefficient monthly mean

Months	\bar{V} (km)	\bar{B} (km)	\bar{b}_{ext} (km^{-1})
January	9.65	0.234	0.436
February	9.30	0.234	0.424
March	14.40	0.226	0.271
April	13.13	0.228	0.316
May	13.06	0.228	0.341
June	13.70	0.227	0.291
July	13.16	0.228	0.307
August	13.80	0.226	0.283
September	13.48	0.227	0.295
October	14.24	0.226	0.275
November	14.06	0.226	0.281
December	9.64	0.235	0.542
Average	12.58	0.229	0.339

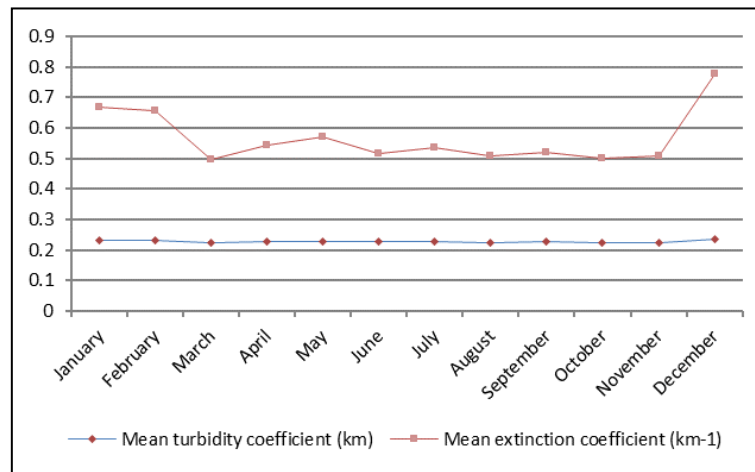


Fig 7: 5-year monthly mean turbidity and extinction coefficient

5. Implications

Turbidity of the atmosphere depends partly on local weather conditions, which determine the input of aerosols from domestic and industrial sources [5]. Based on the analysis, it is observed that Makurdi is generally a hot region with a moderate visibility. However, findings have revealed that the monthly average value of the turbidity coefficient in Makurdi, varies between 0.226 and 0.235. Which implies airplane operation and solar energy utilization. This finding is in line with Lopez and Batlles [5] who gave a range for turbidity coefficient to be between 0.02 for low aerosol load to 0.5 for high aerosol loads. Also, it is similar to Djafer and Irbah [8] evaluation of Angstrom turbidity coefficient between 0.02 and 0.19 but not in line with their monthly average values of Linke turbidity factor of between 1.3 and 5.6. Similarly, the monthly average value of the extinction coefficient ranges from 0.271 in March to 0.542 in December which is similar to Lopez and Batlles [5] but not in line with Djafer and Irbah [8]. However, the extinction coefficient of the atmosphere is proportional to concentration of light absorbing and scattering aerosols in the atmosphere. Since turbidity values determine the input of aerosole loading which have direct effect of scattering and absorbing radiation [11, 5] and our findings have revealed higher aerosole loads during the dry season as compared to the rainy season, it implies that Makurdi will experience more absorption and scattering of solar radiation during the dry season as compared to rainy season.

6. Conclusion

This research work is based on the estimation of mean atmospheric turbidity coefficient in Makurdi. Using the visibility data for the period of five years (2010-2014) from Nigeria Meteorological Headquarters Tactical Air Command Makurdi Airport, the Schuepp method was adapted to measure the atmospheric turbidity coefficient while the Koschmeida method was employed to calculate the extinction coefficient for the city of Markurdi, Nigeria. Though the monthly mean extinction coefficient values were higher than those of turbidity, the monthly mean turbidity coefficients were observed to vary the same way as the extinction coefficient because they both measure the amount of aerosol loading in the atmosphere. The amount of aerosols were observed to vary across the season showing high aerosol loading during the dry season January, February and December and low aerosol loading during the

rainy season. The atmospheric turbidity expresses the attenuation of the solar radiation that reaches the Earth's surface under cloudless sky for technological utilization of solar energy and describes also the optical thickness of the atmosphere for the purposes of meteorology, ecology, climatology and monitoring of atmospheric pollution.

7. Limitations and recommendations

Some limitations of this study are worth mentioning. First a lot of difficulties were encountered in the process of retrieving and analysing the raw data due to monopoly of data and some missing data at the meteorological center. Since only one centre is available in Makurdi, the available data may not fully represent the actual situation of Makurdi. Second, the analysis was only carried out for a period of five years which may not give an excellent result for a time series analysis. Further study with more number of years will give a better result.

8. Funding

This research did not receive any specific grant from funding agencies in the public, commercial, or not-for-profit sectors.

10. References

1. Elminir HK, Rahuma UA, Benda V. Comparism between atmospheric turbidity coefficient of desert and temperate climates. *Acta Polytechnica*. 2001; 41(2):48-59.
2. Robaa SM. Urban-rural solar radiation loss in the atmosphere of Greater Cairo region, Egypt. *Energy Conversion and Management*. 2009; 50(1):194-202.
3. Khalid SA. Parameterization models for solar radiation and solar technology applications. *Energy Conversion and Management*. 2008; 49(1):2384-91.
4. Malik AQ. A modified method of estimating Angstrom's turbidity coefficient of solar radiation model. *Renewable Energy*. 2000; 21(1):537-52.
5. Lopez G, Batlles FJ. Estimate of the atmospheric turbidity from three broad brand solar radiation algorithms. A comparative study. *Annales Geophysicae*. 2004; 22(1):2657-2668.
6. Iqbal M. An introduction to solar radiation. Academic Press. Ontario, Canada, 1983.
7. Rangarajan S, Mani A. A new method for the determination of atmospheric turbidity. *Tellus*. 1984;

- 36B:50-54.
8. Djafer D, Irbah A. Estimation of atmospheric turbidity over Ghardaia city. *Atmospheric Research*, Elsevier. 2013; 128:76-84. [[10.1016/j.atmosres.2013.03.009](#)].<hal-00801475>].
 9. Rahoma AU, Hassan AH. Determination of Atmospheric Turbidity and its Correlation with Climatologically Parameters. *American Journal of Environmental Science*. 2012; 8(6):597-604.
 10. Gueymard AC. Importance of atmospheric turbidity and associated uncertainties in solar radiation and luminous efficacy modeling. Presented at the International Expert Conf. on Measurement and Modeling of Solar Radiation, Edinburgh, 2003, 1-11.
 11. Eltbaakh YA, Ruslan MH, Alghoul MA, Othman MY, Sopain K. Issues concerning atmospheric turbidity indices. *International Journal of Renewable and Sustainable Energy Reviews*. 2012; 16(8):6285-6294.
 12. Stefan S, Iorga G, Zoran M. The atmospheric aerosol and their effects on cloud albedo and radiative forcing. In: *Proceedings of the second environmental physics confer*, Alexandria, Egypt, 2006, 18-22.
 13. Power HC, Willmott CJ. Seasonal and interannual variability in atmospheric turbidity over south-Africa. *International Journal of Climatology*. 2001; 21(1):579-591.
 14. Dutton EG, Reddy P, Ryan S, Deluisi JJ. Features and effects of aerosol optical depth observed at Mauna Loa, Hawaii: 1982-1992. *Journal of Geophysical Research*. 1994; 99(D4):8295-8306.
 15. Holben BN, Eck TE, Slutsker I, Tanre D, Setzer A, Vermot E, Reagan JA, Kaufman YJ, Nakajima T, Lavenu T, Jankowiak I, Smirnov A. AERONET—A Federated instrument network and data archive for aerosol characterization. *Remote Sensing Environment*. 1998; 66(1):1-16.
 16. Tanre D, Herman M, Kaufman YJ. Information on aerosol size distribution contained in solar reflected spectral radiances. *Journal of Geophysical Research*. 1996; 101(D14):19 043-19, 060.
 17. Husar RB, Prospero JM, Stowe LL. Characterization of tropospheric aerosol over the oceans with the NOSAA advanced very high resolution radiometer optical thickness operational product. *Journal of Geophysical Research*. 1997; 102(D14):16, 889-16, 909.
 18. Linke F. Transmission Koeffizient und Trübungs faktor. *Beitr. Phys. Atmos*. 1922; 10:91-103.
 19. Angstrom A. On the atmospheric transmission of sun radiation and in dust in the air. *Geogr. Ann*. 1929; 2:156-166.
 20. Shuepp W. Die Bestimmung der Komponenten der atmosphärischen Trübung aus Aktinometer Messungen. *Arch. Met. Geoph. Biokl. B*. 1949; 1:257-346.
 21. Unsworth MH, Monteith JJ. Aerosols and solar radiation. *Britain Quarterly Journal of the Royal Meteorological Society*. 1972; 98:78-97.
 22. Ganesh KE, Umesh TK, Narasimhamurthy B. Atmospheric turbidity over a continental station Mysore, India. *Indian Journal of Radio and Space Physics*. 2011; 40(1):85-94.
 23. Tendeku F. Retrieval of atmospheric turbidity coefficient and water column density from solar irradiance data. *Journal of Arkansas Academy of Science*, 1995, 49(38).
 24. Katz M, Bailie A, Mermier M. Atmospheric turbidity in a semi-rural site - 1: Evaluation and comparison of different atmosphere turbidity coefficients. *Solar Energy*. 1982; 28:323-327.
 25. Trabelsi A, Masmoudi M. An investigation of atmospheric turbidity over Kerkennah Island in Tunisia. *Atmospheric Research*. 2011; 101:22-30.
 26. Angstrom A. Techniques of determining the turbidity of the atmosphere. *Tellus*. 1961; 13(2):214-223.
 27. Angstrom A. The parameters of atmospheric turbidity. *Tellus*. 1964; 16(1):64-75.
 28. Grenier JC, Adelcasme C, Cabot T. A spectral model of Linke's turbidity factor and it's experimental implication. *Solar Energy*. 1994; 52:303-313.
 29. Alnaser WE, Awadalla SN. The link's turbidity factor and Angstrom coefficient in humid climate of Bahrain. *Earth, Moon and Planets*. 1995; 70(1-3):61-74.
 30. Majumuda NG, Garg OP, Agarwal BK. Further study on rational turbidity factor at unit airmass. *Defence Science Journal*. 1979; 29(1):35-8.
 31. Navvab M, Karayel M, Neec E, Selkowitz S. Analysis of atmospheric turbidity for daylight calculations. *Energy and Buildings*. 1984; 6:293-303.
 32. Abdelrahman MA, Said SAM, Shuaib AN. Comparison between atmospheric turbidity coefficient of desert and temperate climate. *Solar energy*. 1998; 40(3):219-225.
 33. Adeyefa ZD, Adedokun JA. Pyrheliometric determination of atmospheric turbidity in harmattan season over Ile-Ife, Nigeria. *Renewable Energy*. 1990; 1(3-4):555-566.
 34. Kastrov VG. On the basic actinometric formula. *Meteorological Bulletin*, 1928, 7.
 35. Excell RHB. The intensity of solar radiation. A publication of King Mongkuts University of Technology, Thonburi, 2000, 3.
 36. Dobbins RA. Atmospheric motion and air pollution. Wiley interscience, New York, 1979, 192.